Received: 24 May 2022 | Revised: 3 August 2022 | Accepted: 11 September 2022

DOI: 10.1002/bit.28237

ARTICLE

BIOTECHNOLOGY AND BIOENGINEERING WILEY

Scalable manufacturing platform for the production of PEGylated heme albumin

Chintan Savla | Andre F. Palmer

William G. Lowrie Department of Chemical and Biomolecular Engineering, The Ohio State University, Columbus, Ohio, USA

Correspondence

Andre F. Palmer, William G. Lowrie Department of Chemical and Biomolecular Engineering, The Ohio State University, 452 CBEC, 151 West Woodruff Ave, OH 43210, USA.
Email: palmer.351@osu.edu

Funding information

R01HL126945; National Institutes of Health; R01HL159862; R01HL158076; R01HL156526; R01HL138116; R01EB021926; R01HL162120

Abstract

Cell-free heme, which was previously shown to have adverse effects on the innate immune system, does not induce inflammation when bound to a protein carrier via overexpression of the enzyme heme-oxygenase 1 (HO-1). Studies in mouse macrophage cell culture and human endothelial cells have confirmed HO-1 catalyzed breakdown of protein bound heme into biliverdin, iron, and carbon monoxide (CO), which elicits anti-inflammatory effects. However, to fully realize the anti-inflammatory therapeutic effects of heme, a colloidally stable heme protein carrier must be developed. To accomplish this goal, we incorporated multiple heme molecules into human serum albumin (HSA) via partial unfolding of HSA at basic pH followed by refolding at neutral pH, and subsequently conjugated the surface of the heme-HSA complex with polyethylene glycol (PEG) to stabilize heme-HSA. Quantification studies confirmed that a maximum of 5–6 hemes could be bound to HSA without precipitation or degradation of heme-HSA. Dynamic light scattering, size exclusion-high performance liquid chromatography (SEC-HPLC), and matrix-assisted laser desorption/ionization time-of-flight (MALDI-TOF) mass spectrometry confirmed the increase in hydrodynamic diameter and molecular weight (MW), respectively, upon PEGylation of heme-HSA. Furthermore, PEG-heme-HSA was stable upon exposure to different pH environments, freeze-thaw cycles, and storage at 4°C. Taken together, we devised a synthesis and purification platform for the production of PEGylated heme-incorporated HSA that can be used to test the potential anti-inflammatory effects of heme in vivo.

KEYWORDS

anti-inflammatory drug, PEGylation, protein purification, scalable purification, surface modification

1 | INTRODUCTION

The effects of free heme on the innate immune system following exposure to cell-free hemoglobin (Hb) have been studied extensively (Larsen et al., 2010; Nathan, 2002; Porto et al., 2007). However, a recent study challenged the assumption that heme is a major proinflammatory mediator in vivo by demonstrating that protein-associated heme or Hb did not induce inflammatory gene expression over a broad range of exposure conditions, which was corroborated in human endothelial cell culture as well as mouse macrophage cell

culture (Vallelian et al., 2018). Other studies observed that heme elicits anti-inflammatory effects, by promoting overexpression of heme-oxygenase 1 (HO-1), which catalyzes the breakdown of heme into biliverdin, iron and carbon monoxide (CO) (Janciauskiene et al., 2020; vet Hanspeter Nägeli, 2018; Vijayan et al., 2018). HO-1 is upregulated in response to various stimuli, including pro-oxidants and pro-inflammatory mediators (Xu et al., 1999). Hence, the therapeutic potential of HO-1 induction to treat chronic inflammatory and autoimmune diseases is an exciting area of research. Existing strategies to harness the therapeutic potential of HO-1 include phytochemicals and HO-1 inducers (Vijayan et al., 2018). Hence it is possible to utilize heme as an HO-1 inducer, thus catalyzing the production of carbon monoxide (CO) and biliverdin, which should result in anti-inflammatory effects. Heme is a highly hydrophobic molecule, and is mainly soluble in organic solvents or basic aqueous solutions (Stiebler et al., 2010). Therefore, to increase heme's aqueous solubility, colloidal stability, and anti-inflammatory therapeutic potential, this current study will take advantage of heme's ability to bind to the ubiquitous plasma protein human serum albumin (HSA) under basic conditions, and then covalently link poly (ethylene glycol) (PEG) to the surface of the heme-HSA conjugate to form PEGylated heme-HSA (PEG-heme-HSA). This strategy first increases the aqueous solubility of heme by binding it to a carrier protein (HSA) that itself is soluble in aqueous solution, and then subsequently further improves the colloidal stability of heme-HSA by PEGylating it. Previously, our lab has stabilized various proteins such as apohemoglobin, and the annelid mega-Hb erythrocruorin via PEG surface conjugation leading to the increased colloidal stability of the PEGylated molecule (Pires et al., 2020; Savla & Palmer, 2021). In this study, we used thiol-maleimide chemistry to facilitate PEGylation of HSA. Surface lysine residues on HSA were reacted with iminothiolane to convert them into thiol groups, which were then reacted with PEG chains (molecular weight [MW] 5000 Da) monofunctionalized with a maleimide reactive group. The conjugation reaction is site-specific and does not produce side products. The unreacted components were then removed via tangential flow filtration (TFF) using a 50 kDa hollow fiber (HF) filter. Therefore, in this study, we investigated heme incorporation into HSA, which was then PEGylated; as well as PEGylation of HSA, followed by heme incorporation on the biophysical properties of the final PEG-heme-HSA product.

2 | EXPERIMENTAL SECTION

2.1 | Materials

25 wt% HSA solution manufactured by Octapharma® was acquired from Nova Biologics. mPEG-maleimide (5000 Da) was purchased from Laysan Bio. Hemin, 5,5-dithio-bis-(2-nitrobenzoic acid) (DTNB), sodium phosphate dibasic (Na_2HPO_4), sodium phosphate monobasic (NaH_2PO_4), sodium chloride (NaCl), potassium chloride (KCl), sodium hydroxide (NaOH), and tris-HCl were purchased from Sigma-Aldrich. TFF modules with a 50 kDa molecular weight cut-off (MWCO) were purchased from Repligen Co. All other chemicals and supplies were purchased from Fisher Scientific.

2.2 | Preparation of Heme-HSA

10 mM hemin stock solution was prepared by dissolving heme in 0.1 M NaOH (Lombardo et al., 2005). 10 ml of 10 mM hemin stock solution was mixed with 15 ml of HSA stock solution at 100 mg/ml and incubated at 37°C for 1 h. The pH of the resulting solution was adjusted to 7.4 using phosphoric acid. The heme-HSA solution was sterile filtered using 0.2 µm filters to remove any large aggregates, and subjected to 10 diafiltration cycles via TFF over a 50 kDa MWCO HF module using phosphate buffered saline (PBS) as the exchange/wash buffer. The preparation of heme-HSA is shown in Figure 1.

2.3 | PEGylation reaction

PEGylation of HSA was performed before and after incorporation of heme using thiol-maleimide chemistry as described in the literature for other proteins (Pires et al., 2020; Savla & Palmer, 2021). For the product heme-PEG-HSA, HSA was incubated with ×2 molar excess of iminothiolane hydrochloride (Fisher Scientific) and ×10 molar excess mPEG-maleimide (5000 Da) (Laysan Bio) at 4°C for 16 h. Unreacted components were removed via diafiltration using TFF HF modules with 50 kDa MWCO in PBS. 4 mM hemin solution in 0.1 M NaOH was then added to PEG-HSA and incubated for 1 h at 37°C. TFF was performed again to remove excess reagents. For the product PEG-heme-HSA, heme-HSA was prepared as described previously. PEGylation was carried out by incubating heme-HSA with ×2 excess iminothiolane and ×10 excess mPEG-maleimide (5000 Da). TFF was performed to remove unreacted components. All final materials were filtered through 0.2 µm syringe filters and stored at −80°C. The preparation of PEG-heme-HSA is shown in Figure 1.

2.4 | Total protein measurement

The concentration of HSA was determined by UV-visible spectrometry using an extinction coefficient of 35,700 $M^{-1}\,cm^{-1}$ at 280 nm (Akbarzadehlaleh et al., 2016; Pace et al., 1995). Spectrophotometric absorbance measurements were obtained using a HP 8452A diode array spectrophotometer (Olis).

2.5 | Thiol quantification assay

A stock solution of 5,5-dithio-bis-(2-nitrobenzoic acid) (DTNB) was diluted 50 times in reaction buffer (0.1 M sodium phosphate, 1 mM ethylenediaminetetraacetic acid pH 8.0) to yield a 0.2 mM working solution of DTNB. Protein samples were diluted to 1–4 mg/ml in reaction buffer. 50 µl of protein sample was added to 150 µl of

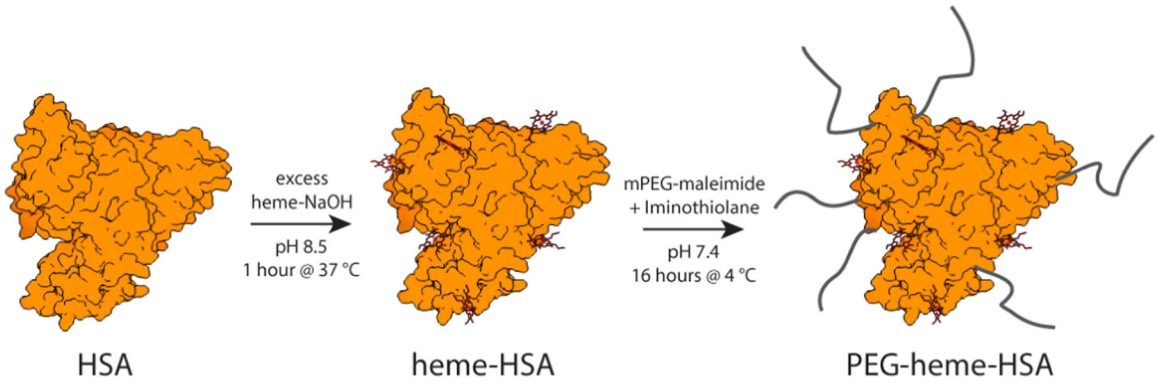

FIGURE 1 Schematic for heme incorporation into HSA and subsequent PEGylation of the protein. Heme was selectively and non-selectively bound to HSA, and the PEG chains were attached to primary surface amines (lysine residues) via thiol-maleimide chemistry. HSA, human serum albumin; PEG, polyethylene glycol.

DTNB working solution and allowed to react for 2 min. Absorbance readings were taken in a micro well plate reader at 412 nm. The readings were adjusted for the initial absorbance, and the concentration of thiols in the sample was determined using an extinction coefficient of 14,100 M^{-1} cm^{-1} at 412 nm (Winther & Thorpe, 2014).

2.6 | Heme incorporation quantification

Heme-HSA was synthesized as previously described at varying heme to HSA molar ratios—×2, ×6, ×10, and ×12. Samples of HSA were collected at multiple points in the synthesis process—pre-reaction HSA pH 7.0, heme-NaOH + HSA start of reaction pH 8.5, heme-NaOH + HSA end of reaction pH 8.5, heme-NaOH + HSA pH 7.4, and final product heme-HSA pH 7.4 after TFF diafiltration. All final products were centrifuged at 20,000 *g* for 3 min to precipitate unbound heme. The supernatant was removed, and the heme pellet was solubilized in 1 ml of 0.1 M NaOH. The concentration of unbound heme (i.e., from NaOH solubilized heme pellet) in each sample was determined using the absorbance at the 398 nm peak, and using an extinction coefficient of $12 \times 10^4 M^{-1}$ cm^{-1} (Lombardo et al., 2005). The difference in the mass of free heme solubilized in NaOH before reaction (total heme), and after centrifugation to form the heme pellet (unbound heme) was used to determine the amount of bound heme in the heme-HSA sample.

2.7 | Quaternary structure

Samples were separated on an analytical Acclaim size exclusion chromatography (SEC)-1000 (4.6 × 300 mm) column (Thermo Fisher Scientific) attached to a Dionex UltiMate 3000 UHPLC/HPLC system (Thermo Fisher Scientific). The mobile phase consisted of 50 mM sodium phosphate buffer at pH 7.4. Chromeleon 7 software was used to control high performance liquid chromatography (HPLC) parameters such as flow rate (0.35 ml/min), UV-visible absorbance detection (280 and 398 nm), and fluorescence detection (excitation at 285 nm, emission at 330 nm). All samples were filtered through 0.2 µm syringe filters before size exclusion HPLC (SEC-HPLC) analysis.

2.8 | Hydrodynamic diameter

The hydrodynamic diameter of protein samples was measured using a BI-200SM goniometer (Brookhaven Instruments Corp.) at an angle of 90° and wavelength of 637 nm. Protein samples were diluted to ~0.5–1 mg/ml concentration in deionized water. The hydrodynamic diameter was obtained by using average values from the nonlinear least squared algorithm in the instrument software.

2.9 | Secondary structure

The far UV circular dichroism (CD) spectra of protein samples was measured using a JASCO J-815 CD (JASCO) spectrometer. Samples were diluted to 10 µM (protein basis) in deionized water and the absorbance was measured from 200 to 260 nm. For each measurement, spectra were obtained by averaging 3 repeated scans. Baseline subtraction was performed, and the absorbance was normalized using the protein concentration. The molar ellipticity was reported in units of deg cm^2 $dmol^{-1}$. The α-helix peak at 222 nm was used to determine the change in α-helical content of samples.

2.10 | Mass spectral analysis

Samples were diluted to 0.5 mg/ml on a protein basis in deionized water. A saturated solution of α-cyano-4-hydroxycinnamic acid (CHCA) matrix was prepared in 50% v/v acetonitrile with 0.1% trifluoroacetic acid (TFA). One microliter of the mixture of the matrix and protein solution was deposited on a matrix assisted laser desorption/ionization (MALDI) plate and run on a Microflex matrix-assisted laser desorption/ionization time of flight (MALDI-TOF) mass

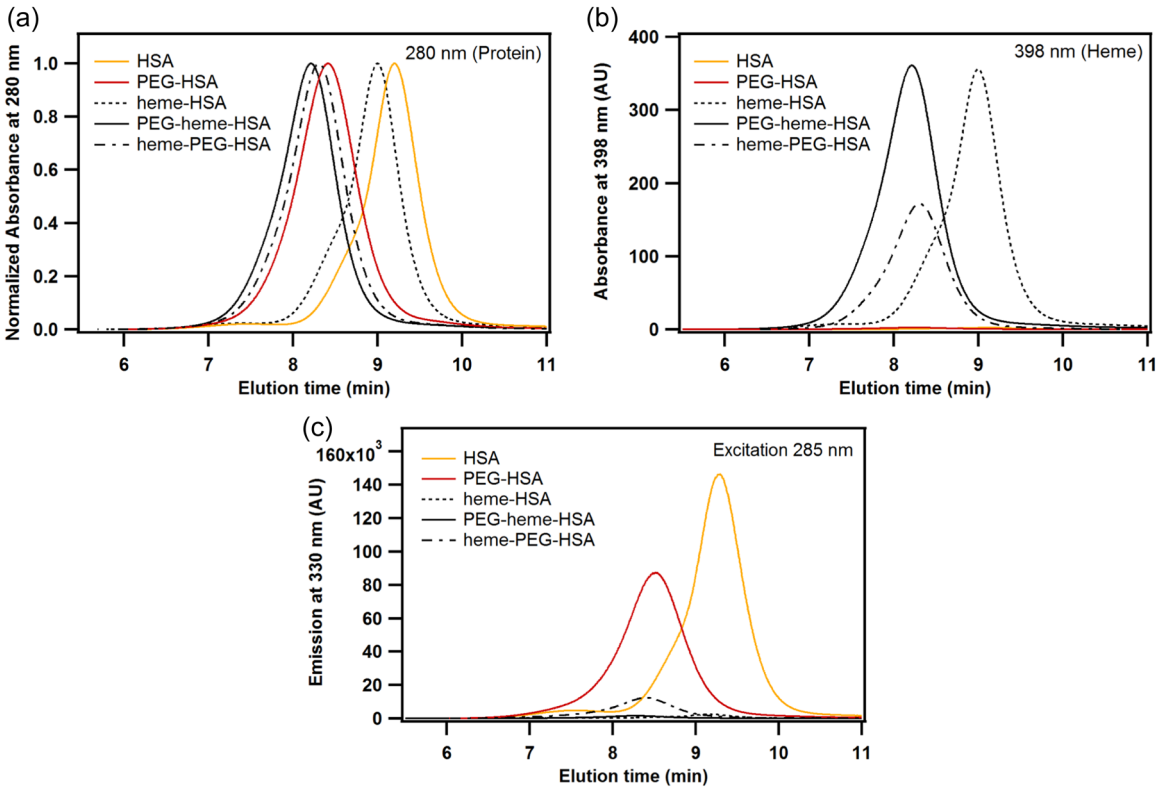

FIGURE 2 SEC-HPLC analysis of HSA, heme-HSA, PEG-HSA, PEGylated heme-HSA (PEG-heme-HSA), and heme incorporated PEG-HSA (heme-PEG-HSA). (a) Normalized absorbance at 280 nm (detects total protein). (b) Absorbance at 398 nm (detects heme). (c) Fluorescence emission at 330 nm after excitation at 285 nm (heme incorporation quenches protein fluorescence). HSA, human serum albumin; PEG, polyethylene glycol; SEC-HPLC, size exclusion high performance liquid chromatography.

spectrometry system (Bruker). The data was analyzed using Flex Analysis software (Bruker).

2.11 | Stability analysis

Heme-HSA and PEG-heme-HSA samples were either stored at 4°C, or −80°C. Frozen samples (−80°C) were thawed at room temperature and stored at 4°C for 0, 24, and 72 h to test for structural changes caused by the freeze-thaw cycle and extended storage at 4°C. All samples were subjected to SEC-HPLC analysis as previously described. Elution times of the peaks and respective areas under the curve were quantified to determine the structural stability of the products when stored at room temperature and after exposure to a freeze-thaw cycle.

2.12 | Transfer reaction

Equimolar solutions of HSA were prepared in PBS. PEG-Heme-HSA was incubated with HSA at the following molar ratios 1:20, 1:50, and 1:75 to replicate potentially therapeutic levels of PEG-Heme-HSA in the circulation. PEG-Heme-HSA and HSA were thoroughly mixed and incubated at 37°C for 48 h. SEC-HPLC analysis was performed at 1 and 48 h time points. Absorbance readings were collected at 280 nm (to detect total protein) and 398 nm (to detect the heme prosthetic group) and fluorescence readings were collected for excitation at 285 nm and emission at 330 nm which detects the ability of heme to quench the fluorescence of HSA. The change in the area under the curve (AUC) for the PEG-Heme-HSA peak and the HSA peak was used to determine the transfer of heme from PEG-Heme-HSA to HSA.

2.13 | Statistical analysis

In this study, all statistical analysis was performed using analysis of variance (ANOVA) tests, and a p value of <0.05 was considered significant.

3 | RESULTS AND DISCUSSION

To analyze the incorporation of heme into HSA, SEC-HPLC analysis was performed as shown in Figure 2. The MW of the protein was inversely proportional to the elution time from the column. HSA eluted from the column at 9.2 min, whereas heme-HSA eluted earlier at ~8.9 min indicating successful heme incorporation. Conversion of

elution time to MW using MW standards suggested that HSA had a MW of 66 kDa, whereas heme-HSA had a MW of ~71 kDa. Furthermore, no peaks were observed at ~13 min, which corresponded to the presence of free heme (616 Da), and hence confirmed that TFF diafiltration and 0.2 µm syringe filtration was successful in removing any free heme or heme aggregates. Successful PEGylation of HSA was confirmed as the elution time of PEG-HSA was 8.4 min, which corresponded to a MW of ~130 kDa. Based on thiol quantification assays, we estimated that ~5 PEG chains were attached to each HSA molecule resulting in a positive MW change of ~25 kDa compared to HSA. The SEC-HPLC elution time to MW conversion, however, suggested that the MW change was ~64 kDa. This discrepancy is expected as it has been reported previously that PEG conjugation exaggerates the MW change of conjugated proteins analyzed via SEC-HPLC due to the large hydration radius of the PEG conjugated molecules (Mehtala et al., 2015; Vandegriff et al., 2008).

To incorporate heme in PEG-HSA, two approaches were used. First, heme was incorporated into previously PEGylated HSA. Second, heme was incorporated into HSA followed by PEG surface conjugation. The subsequent products were referred to as heme-PEG-HSA and PEG-heme-HSA, respectively. The elution time of heme-PEG-HSA was ~8.2 min, whereas it was ~8.1 min for PEG-heme-HSA corresponding to a MW of ~140 and ~154 kDa respectively. This initially suggested that more heme was incorporated into HSA when PEGylation was performed after heme incorporation into HSA. Furthermore, for the same concentration of protein, the 398 nm absorbance peak area (detects heme) was ~265 mAU*min for heme-HSA, 273 mAU*min for PEG-heme-HSA, and 146 mAU*min for heme-PEG-HSA. Note that no absorbance at 398 nm was observed for HSA and PEG-HSA, as none of these species had heme incorporation. Since the total protein concentration is directly proportional to the absorbance area under the curve (AUC), this confirmed that less heme was incorporated into PEGylated HSA than unPEGylated HSA. This result was expected as the steric hindrance caused by PEG chain conjugation on the surface of HSA allows less heme to be incorporated in the hydrophobic binding pockets of the protein. To further confirm these results, the excitation/emission spectra was measured at 285/330 nm respectively. Heme, among other metal-centered porphyrins, is known to quench the fluorescence of specific amino acid residues by dissipating the energy emitted in its structure (Olson et al., 2017). HSA and PEG-HSA exhibited significant fluorescence, whereas heme-HSA and PEG-heme-HSA had negligible fluorescence due to complete quenching of the fluorescence by the incorporated heme. However, heme-PEG-HSA had some residual fluorescence at 330 nm indicating only partial fluorescence quenching by the incorporated heme. These results confirmed that less heme was incorporated per HSA molecule when heme incorporation was performed after PEGylation of HSA. This further corroborated that the PEG chains created steric hindrance on the outside surface of the HSA molecule allowing less heme to be incorporated. Hence, PEG-heme-HSA was identified as the optimal approach for synthesizing PEGylated heme-HSA, since HSA could incorporate more heme followed by PEGylation.

3.1 | Quantification of bound heme

To determine unbound heme at the final product pH of 7.4, unbound heme was centrifuged to form a pellet, resolubilized in NaOH, and quantified using UV-visible spectroscopy (Figure 3). During heme-HSA synthesis, molar ratios of heme:HSA ranging from 2:1 to 12:1 were investigated. However, it was observed that unbound heme was retained on the 0.2 µm syringe filter. Hence, samples were taken at multiple points during the synthesis process to quantify heme bound to HSA. On initially mixing heme-NaOH with HSA, there were no heme precipitate as all the heme was solubilized in the NaOH solution at pH 8.5. Similarly, no precipitate was observed after incubating the solution at 37°C. When the pH was balanced back to 7.4 using phosphoric acid, a significant pellet of heme was observed for higher heme:HSA molar ratios. Based on the difference between the initial mass of heme and the mass of the pellet, it was concluded that ~5.8 heme molecules were bound to each HSA molecule at a 6:1

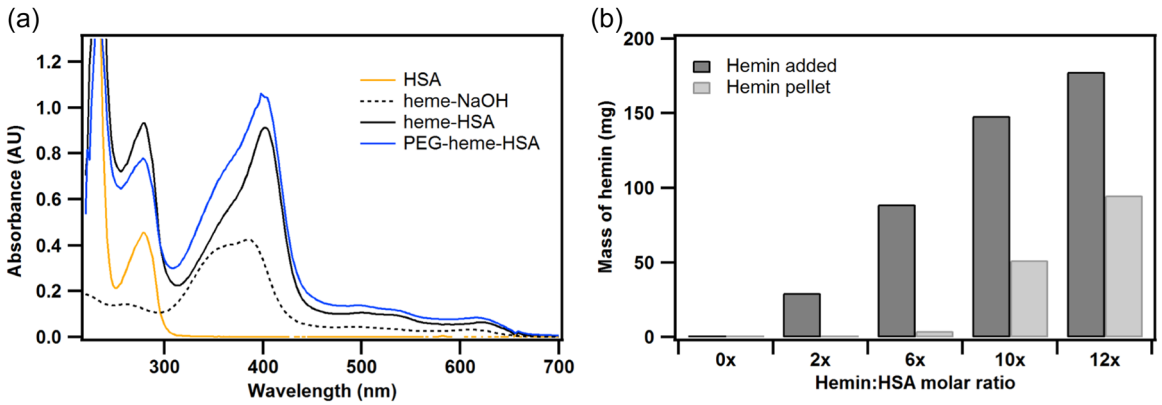

FIGURE 3 (a) UV-visible absorbance spectra of heme-NaOH, HSA, heme-HSA, and PEG-heme-HSA samples. (b) Quantification of heme not bound to HSA. After exceeding a 6:1 heme:HSA molar ratio, the size of the heme pellet significantly increased in mass denoting saturation of the heme binding sites (specific and nonspecific) in HSA. HSA, human serum albumin; PEG, polyethylene glycol.

heme:HSA incubation reaction, 5.3 heme molecules were bound to each HSA molecule at a 10:1 heme-HSA incubation reaction, and 4.9 heme molecules were bound to each HSA molecule at a 12:1 heme-HSA incubation reaction. It is important to note that the maximum amount of heme bound to HSA remained almost constant with increasing heme:HSA molar ratio above 5:1 during synthesis. Hence, it was determined that a maximum of ~5 heme molecules were bound to each HSA molecule at heme:HSA molar ratios > 6:1. Previous studies have shown that HSA has a binding pocket that binds selectively to one heme molecule (Wardell et al., 2002), hence, this study found that ~4 additional heme molecules were nonselectively bound to HSA. It was interesting to note that no heme precipitated out of solution after the reaction, purification, and storage of heme-HSA in aqueous solution at 4°C for over 1 week. Hence, we synthesized a heme-HSA molecule that has ~5 hemes bound per HSA molecule that is stable in aqueous solution without loss or precipitation of heme.

3.2 | Size analysis

Dynamic light scattering (DLS) analysis was performed to determine the change in hydrodynamic diameter of HSA post PEGylation (Figure 4). HSA by itself has a diameter of 3.8 ± 0.4 nm, whereas after heme incorporation it increased to 5.1 ± 2.2 nm, which was significantly different than HSA. The polydispersity index (PDI) of HSA went up from 0.1 to 0.3 post heme incorporation possibly due to the partial unfolding of the HSA structure under the basic pH conditions during heme incorporation. Even after the pH was adjusted to 7.4, it is likely that the HSA did not undergo complete refolding. This hypothesis was tested using CD, and will be discussed later in the

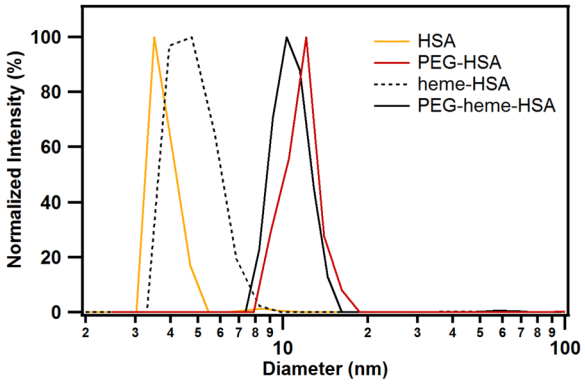

FIGURE 4 Dynamic light scattering (DLS) analysis of HSA and heme-incorporated derivatives. PEGylation resulted in an increase in hydrodynamic diameter of HSA and heme-HSA as expected. HSA, human serum albumin; PEG, polyethylene glycol.

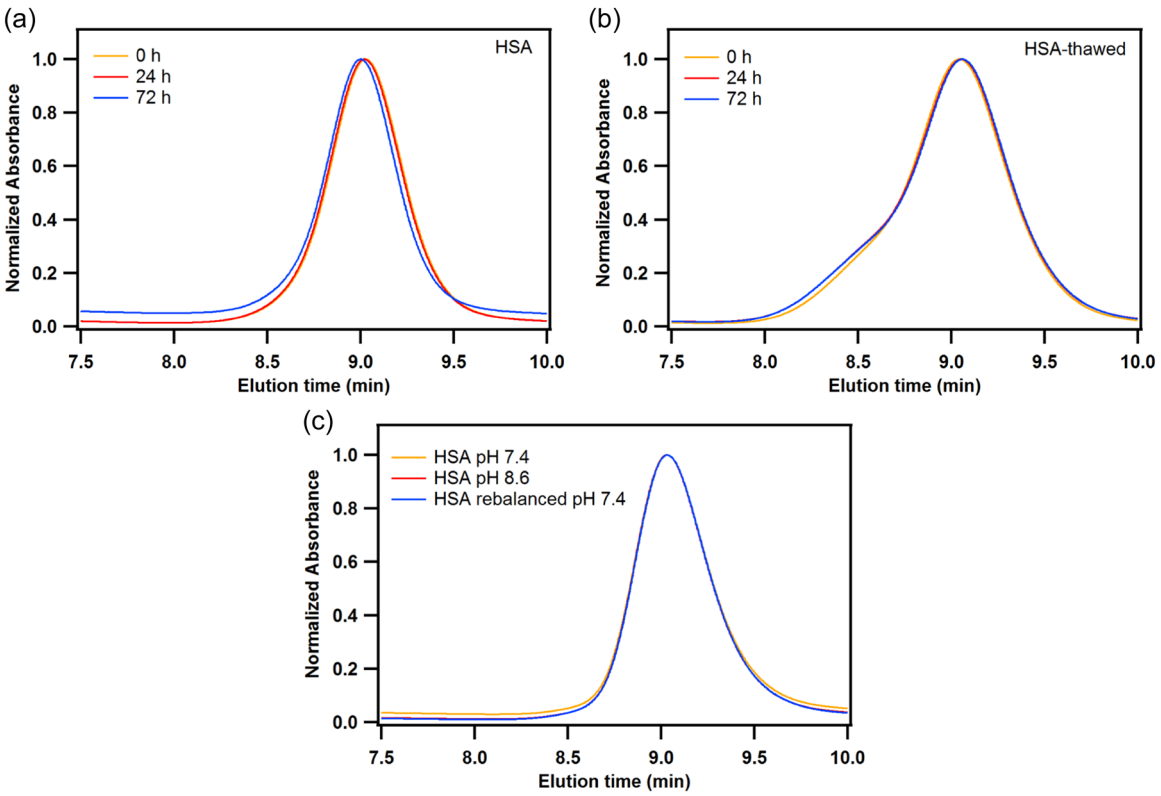

FIGURE 5 SEC-HPLC analysis of (a) HSA and (b) HSA thawed from −80°C storage, and subsequently stored at 4°C for 0, 24, and 72 h. All samples were stable during 72 h of storage, however there was HSA dimer formation after HSA was exposed to a freeze-thaw cycle. (c) SEC-HPLC analysis of HSA samples after undergoing a pH shift from 7.4 to 8.6 and rebalancing to 7.4. No change in the quaternary structure was observed throughout the pH balancing process. HSA, human serum albumin; SEC-HPLC, size exclusion high performance liquid chromatography.

results and discussion section. Upon PEGylation of HSA, the hydrodynamic diameter increased to 13.1 ± 0.6 nm confirming successful PEG surface conjugation. This was also statistically significant compared to HSA. Upon PEGylation of heme-HSA, the diameter increased from 5.1 ± 1.2 to 11.9 ± 1.4 nm, which was statistically significant, and the PDI was reduced from 0.3 to 0.2. Interestingly, there was no statistically significant difference in the diameter of PEG-HSA and PEG-heme-HSA. DLS analysis confirmed the results from SEC-HPLC that there was successful PEGylation of the HSA molecule before and after heme-incorporation. Furthermore, there were no other species detected in the DLS analysis denoting no free heme or aggregated heme particulates. PEG conjugation has previously been shown to result in similar diameter changes for proteins such as hemoglobin and apohemoglobin, which also improved the colloidal stability of the proteins in aqueous solution (Hu et al., 2005; Lawrence & Price, 2016; Smani, 2008).

3.3 | Storage stability

To further test the colloidal stability of PEGylated heme-HSA in storage, all samples were tested under multiple storage conditions (Figures 5, 6). Samples were either stored at 4°C for 72 h with periodic SEC-HPLC measurements or frozen at −80°C, thawed, and then stored at 4°C. These conditions were selected to simulate storage of the product for future use in in vivo experiments that will evaluate the anti-inflammatory effects of protein bound heme. HSA did not exhibit any changes in quaternary structure after storage at 4°C for 72 h but showed ~15% dimerization (elution time ~8.4 min) upon exposure to a single freeze-thaw cycle and subsequent storage at 4°C for 72 h. Furthermore, no change in the quaternary structure of HSA was observed in the pH rebalancing process. Upon storage of heme-HSA at 4°C, there was no change in the SEC-HPLC elution profile for ~24 h, but there was the appearance of dimeric species (elution time ~8.4 min) after 72 h indicating protein aggregation. PEG-heme-HSA was very stable throughout the 72 h storage period at 4°C, and did not show any change in the SEC-HPLC elution profile. Post one freeze-thaw cycle, heme-HSA yielded the appearance of >20% larger species (~8.4 min) at 0 h, which increased to ~90% larger species after 72 h of storage at 4°C. Since we expect the HSA molecule to partially unfold under the basic conditions used for heme incorporation and refold after rebalancing to pH 7.4, its' structural stability is potentially compromised, which is further exaggerated following exposure to a single freeze thaw cycle. However, post PEGylation, the protein structure was stabilized, and we observed no change in the quaternary structure of PEGylated heme-HSA directly

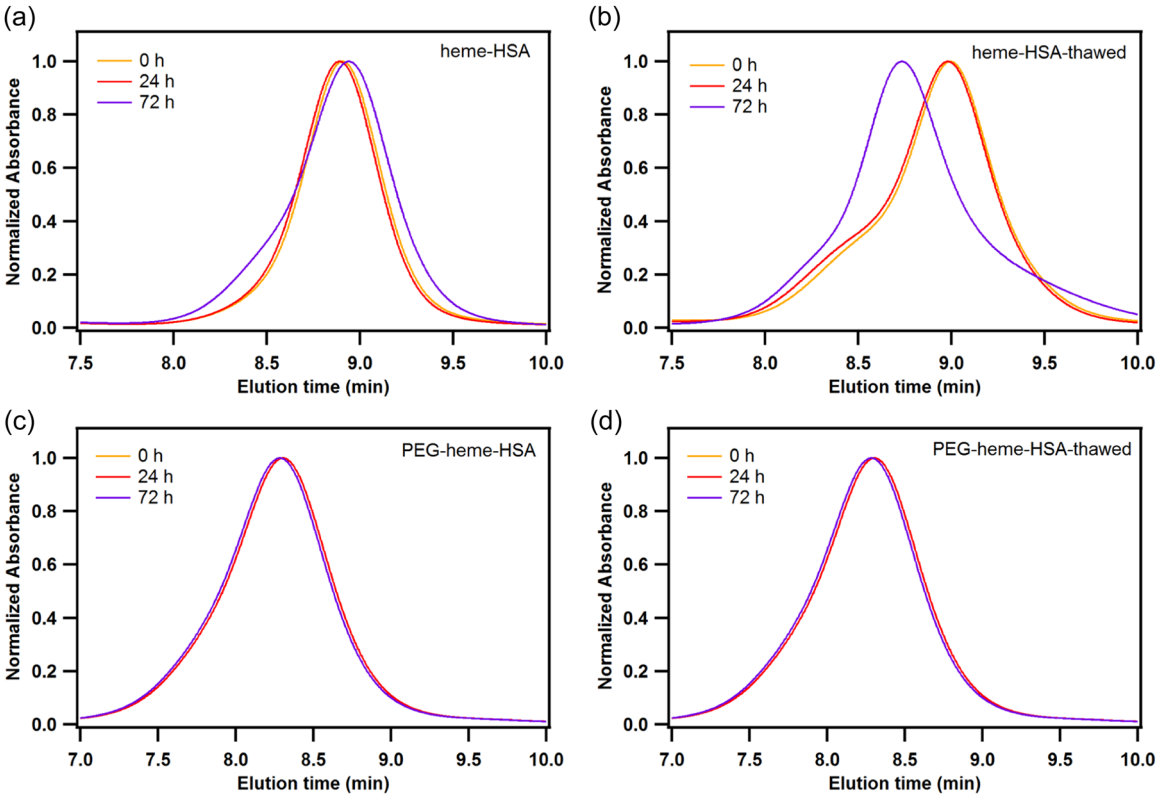

FIGURE 6 Storage stability of heme-HSA and PEG-heme-HSA. (a, c) SEC-HPLC analysis of heme-HSA and PEG-heme-HSA stored at 4°C for 0, 24, and 72 h. (b, d) SEC-HPLC analysis of heme-HSA and PEG-heme-HSA samples frozen at −80°C, thawed at 4°C, and stored for 0, 24, and 72 h at 4°C. PEGylated samples demonstrated higher colloidal stability and no change in quaternary structure during 72 h storage, whereas unPEGylated heme-HSA showed dimer formation after 24 h in storage and after exposure to a single freeze thaw cycle. HSA, human serum albumin; PEG, polyethylene glycol; SEC-HPLC, size exclusion high performance liquid chromatography.

post a single freeze-thaw cycle, and after 72 h of storage at 4°C. This further supports the increased colloidal stability of PEG-heme-HSA, and justified the use of PEG as a suitable molecule for heme-HSA surface conjugation and stabilization. Furthermore, it was important to note that no free heme aggregates were observed in all samples post exposure to a single freeze-thaw cycle.

3.4 | Heme transfer reaction

The SEC-HPLC elution peaks at 280 nm confirmed the fixed HSA concentration (elution time: 9.4 min) in each sample and the different concentrations of PEG-heme-HSA (elution time: 8.7 min) used in the experiments (Figure 7). All comparisons between HSA and PEG-heme-HSA mixtures were made between 0 and 48 h samples. There was no change in total protein over 48 h, which confirmed that the products were colloidally stable at 37°C over that time period. The heme bound to PEG-heme-HSA or HSA was monitored via the absorbance at 398 nm. For all 3 ratios of HSA to PEG-heme-HSA, the initial amount of heme (determined by the AUC) at 0 h for the PEG-heme-HSA peak reduced by <12% over 48 h. An equivalent increase in AUC for the HSA peak which eluted at 9.4 min was indicative of heme transfer from PEG-heme-HSA to HSA. Initially (t = 0 h), the HSA elution peak had no absorbance at 398 nm (~0 mAU), which increased to 14 mAU for the molar ratio 1:20, 6 mAU for the molar ratio 1:50, and 5 mAU for the molar ratio 1:75. This confirms the transfer of heme from PEG-heme-HSA to HSA over 48 h at 37°C. However, the transfer of heme was <12% in all cases, which indicated that the majority of the heme was still bound to PEG-heme-HSA, although nonselectively as shown earlier. This was further confirmed via the fluorescence emission at 330 nm. Upon transfer of heme to HSA, we observed a reduction in the fluorescence of HSA at 9.4 min, since heme binding to HSA quenches the fluorescence. It is important to note that PEG-heme-HSA had no emission peak at 8.7 min as the heme quenched all the fluorescence. The changes in fluorescence AUC suggested that as compared to the HSA peak at time 0 h, the fluorescence reduced by ~18% for the molar ratio 1:20, ~11% for the molar ratio 1:50, and ~7% for the molar ratio 1:75. It is also important to note that there was no increase in fluorescence observed for the PEG-heme-HSA peak, which eluted at 8.6 min. Our results confirm that <10% of the total heme cargo was transferred from PEG-heme-HSA to HSA over 48 h at the most therapeutically relevant PEG-heme-HSA to HSA ratios. We do not believe that the transfer of heme to HSA is a major concern for the current product as the transferred heme is more likely to be the non-selectively bound excess heme. To further minimize the transfer of heme to HSA, future synthesis of PEG-heme-HSA can

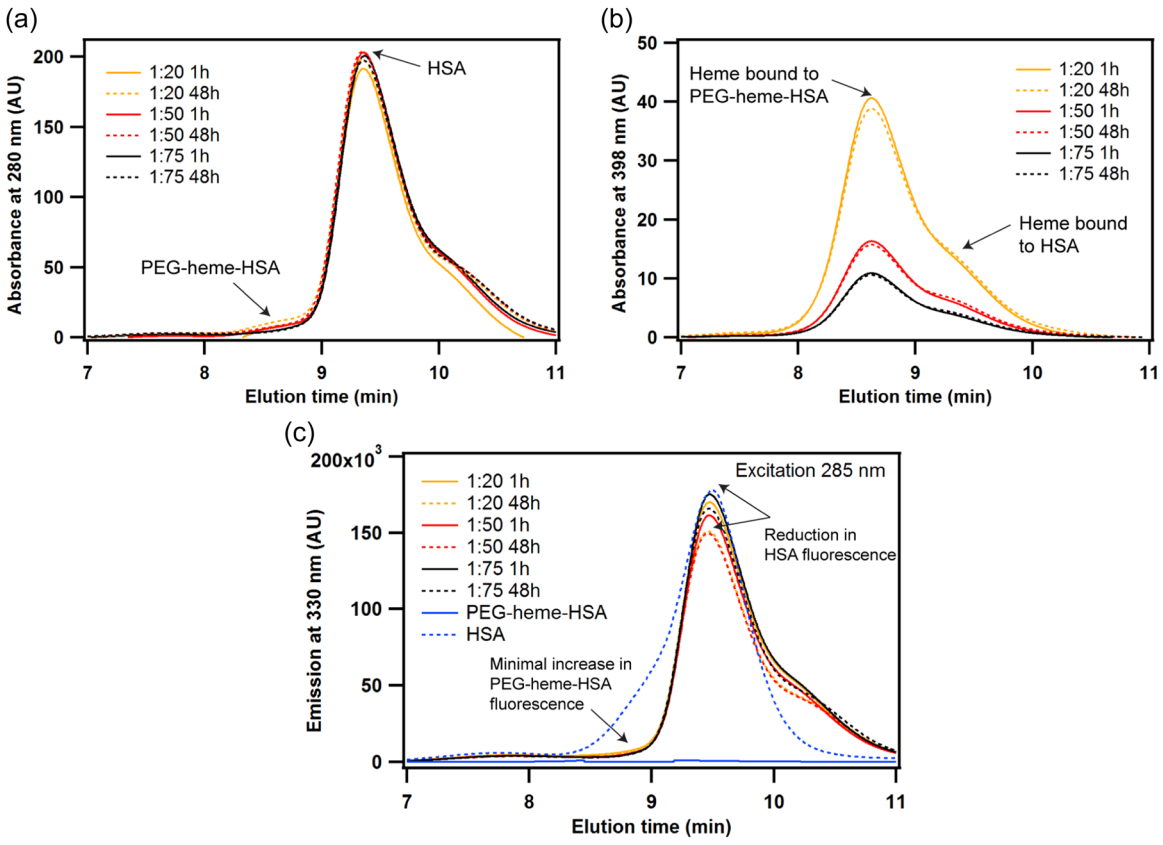

FIGURE 7 Transfer reaction of heme from PEG-heme-HSA to HSA over 48 h assessed via SEC-HPLC. (a) Absorbance at 280 nm indicative of total protein. (b) Absorbance at 398 nm indicative of heme. (c) Fluorescence emission at 330 nm after excitation at 285 nm. HSA, human serum albumin; PEG, polyethylene glycol; SEC-HPLC, size exclusion high performance liquid chromatography.

be tuned by reducing the amount of non-selectively bound heme to PEG-heme-HSA.

3.5 | Secondary structure modifications

The change in α-helical content of HSA during heme-incorporation and postmodification was monitored using CD spectroscopy (Figure 8). The peak at 222 nm was used to monitor the change in α-helical content. The different intermediates are as follows: Intermediate 1—Heme-NaOH + HSA start of reaction pH 8.5; Intermediate 2—Heme-NaOH + HSA end of reaction pH 8.5; and Intermediate 3—Heme-NaOH + HSA pH balanced to 7.4. HSA has a hydrophobic pocket that selectively binds to one heme molecule. However, it also has nonselective heme-binding sites as confirmed via the heme pellet centrifugation quantification study. The α-helical content of heme-HSA intermediates 1 and 2 was reduced by ~38% compared to HSA denoting partial unfolding of the HSA secondary structure under the basic conditions used for heme incorporation as hypothesized (Figure 8, center). The α-helical content of intermediate 3 and heme-HSA then increased to ~80% of the original HSA α-helical content after balancing the pH back to 7.4 using phosphoric acid. It is interesting to observe that there was a permanent change in the secondary structure of HSA after heme incorporation as the α-helical content did not recover to that of the original HSA. This is consistent with HSA by itself which undergoes a ~60% reduction in α-helical content after a pH change to 8.6, which does not fully recover after rebalancing the pH to 7.4 (Figure 8, left). After PEG-conjugation, the α-helical content reduced by ~9% compared to heme-HSA indicating no major changes to the heme-HSA secondary structure after the PEGylation process (Figure 8, right). These results confirmed the hypothesis that there was partial unfolding of the HSA molecule under the basic pH conditions conducive to heme incorporation, and subsequent partial refolding when the pH was adjusted back to 7.4.

3.6 | Mass spectroscopy analysis

The change in the MW of HSA post PEGylation was verified using MALDI-TOF mass spectral analysis (Figure 9). The HSA control showed characteristic peaks at ~66,000 m/z (+1 charged species), ~33,000 m/z (+2 charged species), ~22,000 (+3 charged species), etc. Upon PEGylation, the m/z shifted to ~80,000 m/z for the +1 charged species confirming successful surface modification of HSA. There was also the presence of multiply charged peaks at ~39,000,

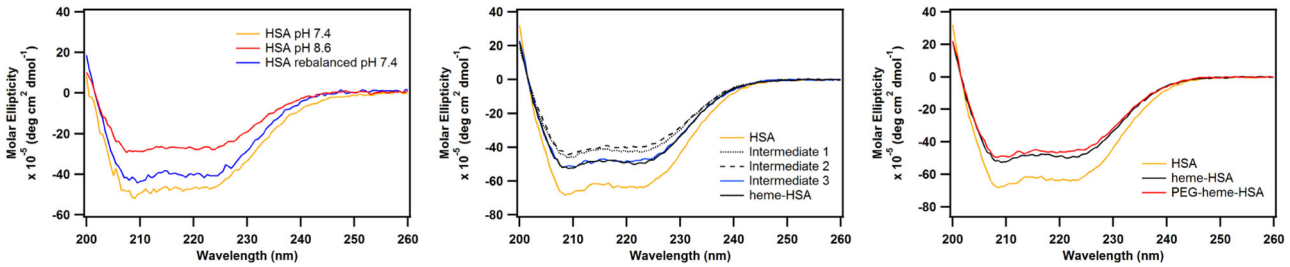

FIGURE 8 CD analysis of HSA (left), heme-HSA intermediates (center), and PEG-heme-HSA (right). Samples were collected at different points during the synthesis process to monitor the α-helical content of HSA. Intermediate 1—Heme-NaOH + HSA start of reaction pH 8.5; Intermediate 2—Heme-NaOH + HSA end of reaction pH 8.6; Intermediate 3—Heme-NaOH + HSA pH balanced to 7.4; heme-HSA final product pH 7.4 after diafiltration; PEG-heme-HSA final product pH 7.4 after diafiltration. HSA, human serum albumin; PEG, polyethylene glycol.

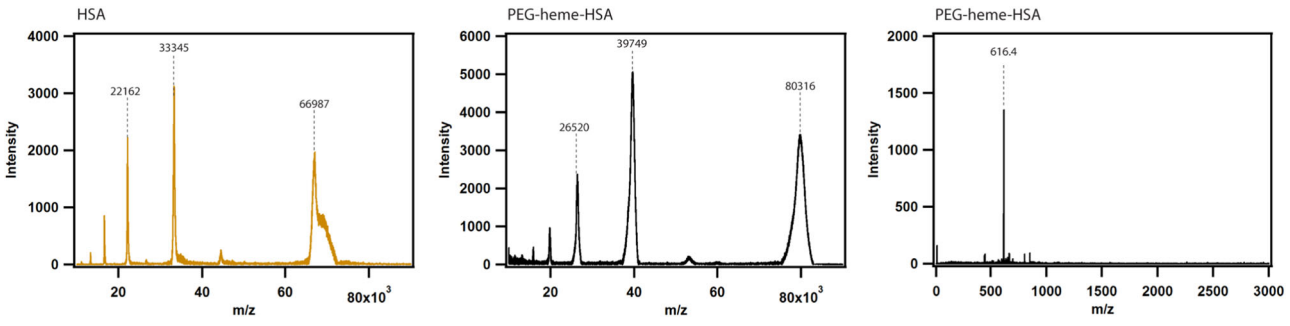

FIGURE 9 MADLI-TOF mass spectral analysis of HSA and PEG-heme-HSA samples. HSA showed a characteristic single-charged peak at ~66,000 m/z along with +2 and +3 charged species. Post-PEGylation, the single charged species shifted to ~80,000 m/z denoting successful surface conjugation. A 616 m/z peak was also observed denoting the presence of heme and its' successful incorporation into HSA. HSA, human serum albumin; PEG, polyethylene glycol.

~26,000 m/z, etc. Furthermore, at the lowest m/z range, there was also the presence of a characteristic heme peak at 616 m/z denoting the presence of heme and its' incorporation into the protein. Comparing MALDI-TOF mass spectral analysis with SEC-HPLC MW estimates, the MW of PEG-heme-HSA was lower by ~40 kDa. It has previously been reported that the PEG chains create a large hydration shell around the protein, which in turn exaggerates the MW estimates after SEC-HPLC analysis. This analysis combined with results from thiol quantification analysis concluded that ~4 PEG chains were conjugated to the surface of each HSA molecule along with 1 specifically bound heme and ~4 heme molecules nonspecifically bound to the PEG-heme-HSA molecule.

4 | CONCLUSION

In conclusion, we successfully incorporated heme into HSA followed by PEGylation to synthesize a colloidally-stable product that can be used in future studies to test the anti-inflammatory effects of heme in vitro and in vivo. The incorporation of heme into HSA followed by surface PEGylation was shown to incorporate more heme versus incorporating heme into already PEGylated HSA as confirmed by SEC-HPLC, UV-visible analysis at 280 nm (to detect protein), 398 nm (to detect hemin), and fluorescence detection at 330 nm (to detect fluorescence quenching of incorporated heme). Furthermore, the increase in MW and hydrodynamic diameter of PEG-heme-HSA versus HSA was confirmed using SEC-HPLC and DLS analysis respectively. CD analysis confirmed the partial unfolding mechanism by which heme was incorporated into HSA, and MALDI-TOF mass spectral analysis confirmed the change in MW before and after surface conjugation of heme-HSA with PEG. Finally, PEG-heme-HSA was found to be more colloidally-stable than heme-HSA, while storing the material at 4°C and after exposure to a single freeze-thaw cycle and subsequent storage at 4 °C for 72 h. Therefore, PEG-heme-HSA is a novel heme carrier that can be used in future in vivo experiments to test the potentially therapeutic anti-inflammatory effects of heme to treat disease.

ACKNOWLEDGMENTS

This study was supported by National Institutes of Health grants R01HL126945, R01HL138116, R01HL156526, R01HL158076, R01HL159862, R01HL162120, and R01EB021926.

DATA AVAILABILITY STATEMENT

The data that support the findings of this study are available from the corresponding author upon reasonable request.

ORCID

Chintan Savla http://orcid.org/0000-0001-7538-8861

REFERENCES

Akbarzadehlaleh, P., Mirzaei, M., Mashahdi-Keshtiban, M., Shamsasenjan, K., & Heydari, H. (2016). PEGylated human serum albumin: Review of PEGylation, purification and characterization methods. *Advanced Pharmaceutical Bulletin*, *6*(3), 309–317. https://doi.org/10.15171/apb.2016.043

Hu, T., Prabhakaran, M., Acharya, S. A., & Manjula, B. N. (2005). Influence of the chemistry of conjugation of poly(ethylene glycol) to Hb on the oxygen-binding and solution properties of the PEG-Hb conjugate. *Biochemical Journal*, *392*(3), 555–564. https://doi.org/10.1042/BJ20050663

Janciauskiene, S., Vijayan, V., & Immenschuh, S. (2020). TLR4 signaling by heme and the role of heme-binding blood proteins. *Frontiers in Immunology*, *11*, 1964. https://doi.org/10.3389/FIMMU.2020.01964/BIBTEX

Larsen, R., Gozzelino, R., Jeney, V., Tokaji, L., Bozza, F. A., Japiassú, A. M., Bonaparte, D., Cavalcante, M. M., Chora, Â., Ferreira, A., Marguti, I., Cardoso, S., Sepúlveda, N., Smith, A., & Soares, M. P. (2010). A central role for free heme in the pathogenesis of severe sepsis. *Science Translational Medicine*, *2*(51), 51ra71. https://doi.org/10.1126/SCITRANSLMED.3001118

Lawrence, P. B. & Price, J. L. (2016). How PEGylation influences protein conformational stability. *Current Opinion in Chemical Biology*, *34*, 88–94. https://doi.org/10.1016/j.cbpa.2016.08.006

Lombardo, M. E., Araujo, L. S., Ciccarelli, A. B., & Batlle, A. (2005). A spectrophotometric method for estimating hemin in biological systems. *Analytical Biochemistry*, *341*(2), 199–203. https://doi.org/10.1016/j.ab.2004.11.002

Mehtala, J. G., Kulczar, C., Lavan, M., Knipp, G., & Wei, A. (2015). Cys34-PEGylated human serum albumin for drug binding and delivery. *Bioconjugate Chemistry*, *26*(5), 941–949. https://doi.org/10.1021/acs.bioconjchem.5b00143

Nathan, C. (2002). Points of control in inflammation. *Nature*, *420*(6917), 846–852. https://doi.org/10.1038/NATURE01320

Olson, K. R., Gao, Y., Arif, F., Arora, K., Patel, S., DeLeon, E., & Straub, K. D. (2017). Innovative methodology: Fluorescence quenching by metal centered porphyrins and poryphyrin enzymes. *American Journal of Physiology— Regulatory, Integrative and Comparative Physiology*, *313*(4), R340-R346. https://doi.org/10.1152/AJPREGU.00202.2017

Pace, C. N., Vajdos, F., Fee, L., Grimsley, G., & Gray, T. (1995). How to measure and predict the molar absorption coefficient of a protein. *Protein Science*, *4*(11), 2411–2423. https://doi.org/10.1002/pro.5560041120

Pires, I. S., Savla, C., & Palmer, A. F. (2020). Poly(ethylene glycol) Surface-conjugated apohemoglobin as a synthetic heme scavenger. *Biomacromolecules*, *21*(6), 2155–2164. https://doi.org/10.1021/acs.biomac.0c00141

Porto, B. N., Alves, L. S., Fernández, P. L., Dutra, T. P., Figueiredo, R. T., Graça-Souza, A. V., & Bozza, M. T. (2007). Heme induces neutrophil migration and reactive oxygen species generation through signaling pathways characteristic of chemotactic receptors. *The Journal of Biological Chemistry*, *282*(33), 24430–24436. https://doi.org/10.1074/JBC.M703570200

Savla, C. & Palmer, A. F. (2021). Structural stability and biophysical properties of the mega-protein erythrocruorin are regulated by polyethylene glycol surface coverage. *Biomacromolecules*, *22*(5), 2081–2093. https://doi.org/10.1021/acs.biomac.1c00196

Smani, Y. (2008). Hemospan: A hemoglobin-based oxygen carrier for potential use as a blood substitute and for the potential treatment of critical limb ischemia. *Current Opinion in Investigational Drugs (London, England)*, *9*(9), 1009–1019. http://www.ncbi.nlm.nih.gov/pubmed/18729008

Stiebler, R., Hoang, A. N., Egan, T. J., Wright, D. W., & Oliveira, M. F. (2010). Increase on the initial soluble heme levels in acidic conditions is an important mechanism for spontaneous heme crystallization in vitro. *PLoS One*, *5*(9), 1–9. https://doi.org/10.1371/JOURNAL.PONE.0012694

Vallelian, F., Schaer, C. A., Deuel, J. W., Ingoglia, G., Humar, R., Buehler, P. W., & Schaer, D. J. (2018). Revisiting the putative role of heme as a trigger of inflammation. *Pharmacology Research & Perspectives*, *6*(2), e00392. https://doi.org/10.1002/prp2.392

Vandegriff, K. D., Malavalli, A., Mkrtchyan, G. M., Spann, S. N., Baker, D. A., & Winslow, R. M. (2008). Sites of modification of hemospan, a poly(ethylene glycol)-modified human hemoglobin for use as an oxygen therapeutic. *Bioconjugate Chemistry*, *19*(11), 2163–2170. https://doi.org/10.1021/bc8002666

vet Hanspeter Nägeli, med. (2018). Heme drives adaptive hypoinflammation in endothelial cells. *Valkova, Kristyna. Heme Drives Adaptive Hypoinflammation in Endothelial Cells. 2018, University of Zurich, Vetsuisse Faculty*. https://doi.org/10.5167/UZH-165484

Vijayan, V., Wagener, F. A. D. T. G., & Immenschuh, S. (2018). The macrophage heme-heme oxygenase-1 system and its role in inflammation. *Biochemical Pharmacology*, *153*, 159–167. https://doi.org/10.1016/J.BCP.2018.02.010

Wardell, M., Wang, Z., Ho, J. X., Robert, J., Ruker, F., Ruble, J., & Carter, D. C. (2002). The atomic structure of human methemalbumin at 1.9 Å. *Biochemical and Biophysical Research Communications*, *291*(4), 813–819. https://doi.org/10.1006/bbrc.2002.6540

Winther, J. R. & Thorpe, C. (2014). Quantification of thiols and disulfides. *Biochimica et Biophysica Acta - General Subjects*, *1840*(2), 838–846. https://doi.org/10.1016/j.bbagen.2013.03.031

Xu, H., Bjerneld, E. J., Käll, M., & Börjesson, L. (1999). Spectroscopy of single hemoglobin molecules by surface enhanced Raman scattering. *Physical Review Letters*, *83*(21), 4357-4360. https://doi.org/10.1103/PhysRevLett.83.4357

How to cite this article: Savla, C., & Palmer, A. F. (2022). Scalable manufacturing platform for the production of PEGylated heme albumin. *Biotechnology and Bioengineering*, 119, 3612–3622. https://doi.org/10.1002/bit.28237